Development 106, 493–509 (1989)
Printed in Great Britain © The Company of Biologists Limited 1989

Characterization of epithelial domains in the nasal passages of chick embryos: spatial and temporal mapping of a range of extracellular matrix and cell surface molecules during development of the nasal placode

S. J. CROUCHER and C. TICKLE

Department of Anatomy and Developmental Biology, University College & Middlesex School of Medicine, Windeyer Building, Cleveland Street, London W1P 6DB, UK

Summary

The formation of the nasal passages involves complex morphogenesis and their lining develops a spatially ordered pattern of differentiation, with distinct domains of olfactory and respiratory epithelium. Using antibodies to the neural cell adhesion molecule (N-CAM), keratan sulphate and heparan sulphate proteoglycan (HSPG) and a panel of lectins (agglutinins of *Canavalia ensiformis* (ConA), *Dolichos biflorus* (DBA), peanut (PNA), *Ricinis communis* (RCA1), soybean (SBA), *Ulex europaeus* (UEA1), and wheatgerm (WGA)), we have documented cell surface characteristics of each epithelial domain. Binding of antibodies to N-CAM and to keratan sulphate, and the lectins ConA, PNA, RCA1, SBA and WGA marks the olfactory epithelial domain only. The restriction of N-CAM to the sensory region of the epithelium has also been reported in the developing ear. This striking similarity is consistent with the idea that N-CAM may be involved in the division of functionally and histologically distinct cell groups within an epithelium.

We traced the olfactory-specific cell markers during development to gain insights into the origin of the epithelial lining of the nasal passages. All reagents bind at early stages to the thickened nasal placode and surrounding head ectoderm and then become progressively restricted to the olfactory domain. The expression of these characteristics appears to be modulated during development rather than being cell autonomous.

The distribution of keratan sulphate was compared with collagen type II in relation to the specification of the chondrocranium. Keratan sulphate and collagen type II are only colocalized at the epithelial–mesenchymal interface during early nasal development. At later stages, only collagen type II is expressed at the interface throughout the nasal passages, whereas keratan sulphate is absent beneath the respiratory epithelium.

Key words: chick embryo, nasal placode, olfactory epithelium, collagen type II, keratan sulphate, heparan sulphate proteoglycan, N-CAM, lectins, ConA, DBA, PNA, RCA1, SBA, UEA1, WGA, differentiation, morphogenesis.

Introduction

The lining of the nose exhibits strikingly different epithelial domains, with the sensory olfactory epithelium in the deeper regions and the nonsensory respiratory epithelium more distally. The development of these two different types of tissue adjacent to each other poses questions about how they are specified and how the boundary between them is defined. This patterned epithelium develops following extensive morphogenesis in the region of the nasal placodes, which are thickenings in the head ectoderm. We wish to understand how the form of the nasal passages arises and, using chick embryos, experimentally determine the mechanisms that lead to epithelial patterning. As a first step towards this long-term goal, we used antibodies to several extracellular and cell surface molecules and a panel of lectins to characterize the epithelial domains in the chick nasal passages.

N-CAM is a cell adhesion molecule that shows interesting spatial and temporal patterns of expression both in early embryos and during organogenesis (reviewed by Edelman, 1985). In the adult, the olfactory epithelium of both mice (Miragall *et al.* 1988) and chickens (Chuong & Edelman, 1984) express N-CAM. During development of the ear, which like the nasal system arises from an ectodermal placode, N-CAM becomes restricted to the sensory regions of the auditory epithelium (Richardson *et al.* 1987). Lectins can also be used to investigate cell surface characteristics. Lectins bind to specific sugars, such as those that are part of membrane-bound glycolipids or of glycoproteins or proteoglycans. In a number of different animals including rodents (Hempstead & Morgan, 1983; Key &

Giorgi, 1986*b*) and frogs (Chen *et al.* 1986; Key & Giorgi, 1986*a*), there is specific binding of lectins within the adult olfactory system. The role of proteoglycans in lectin binding can be evaluated using MZ15, an antibody to keratan sulphate (Smith & Watt, 1985; Zanetti *et al.* 1985) and an antibody to heparan sulphate proteoglycan (Bayne *et al.* 1984).

The distribution of MZ15 staining is also interesting in relation to the 'Fly-paper model' (Thorogood *et al.* 1986; Thorogood, 1988). This model suggests that transient expression of cartilage-specific molecules at epithelial–mesenchymal interfaces in the embryonic head signals the development of the chondrocranium and sensory capsules. The monoclonal antibody, MZ15, recognizes keratan sulphate in both cartilage-specific and noncartilage-specific proteoglycans (Smith & Watt, 1985; Zanetti *et al.* 1985; Mehmet *et al.* 1986). In the chick otic vesicle, an early stage in ear development, there is some degree of colocalization of staining with MZ15 and cartilage-specific type II collagen antibodies (Thorogood, 1988; Heath & Thorogood, 1989). Therefore, we have extended our investigation to include a comparison of the distribution of keratan sulphate and collagen type II during nasal placode development.

Antibodies to N-CAM and keratan sulphate and the lectins ConA, PNA, RCA1, SBA and WGA all recognize the olfactory epithelial domain. These reagents bind to the placode and then become progressively restricted during development.

Materials and methods

Antibodies and lectins

Anti-type-II collagen is an affinity-purified rabbit antibody, produced and kindly donated by Charles Archer (The Institute of Orthopaedics, Stanmore, Middlesex). MZ15 is a mouse monoclonal antibody raised against pig chondrocytes that has been shown to be specific for keratan sulphate (Smith & Watt, 1985; Zanetti *et al.* 1985; Mehmet *et al.* 1986), and was a kind gift from Fiona Watt (Imperial Cancer Research Fund, Lincoln's Inn Fields, London). Anti-heparan sulphate is a monoclonal antibody to heparan sulphate proteoglycan (HSPG) raised against chick embryo leg muscle, from the Developmental Studies Hybridoma Bank, Maryland (NICHD contract number: NO1-HD-6-2915). Biotinylated lectins were obtained from Vector Laboratories. Lectins may bind to any exposed sugar residues in the tissue, such as in glycoproteins, glycolipids or the glycosaminoglycan chains (GAGs) of proteoglycans. However, the density of sugars in such glycoproteins or glycolipids is far lower compared to that in GAGs, which consist of alternating sugar residues; therefore, one can surmise that the lectins are mainly binding to GAGs (Gallagher, 1986). The binding specificities of these lectins and the GAGs to which they are predicted to bind are shown in Table 1. The anti-sera to N-CAM is an Fab fragment of a polyclonal rabbit antibody to N-CAM, which was a generous gift to Mark Noble from Urs Rutishauser (Case Western Reserve School of Medicine, Cleveland, Ohio).

Preparation of tissue

Recently laid, fertilized chicken eggs were incubated in a humidified incubator at 38(±1)°C. Embryos were staged according to Hamburger & Hamilton (1951). Heads were removed in cold phosphate-buffered saline (PBS, 10 mM-sodium phosphate, 0·9% saline, pH 7·5).

Tissue for staining with anti-type-II collagen, anti-HSPG and MZ15, was allowed to sink in 30% sucrose in PBS, embedded in precooled OCT compound (Lab-Tek Products) and frozen in liquid nitrogen. Blocks were cut immediately at −20°C on a Reichert-Jung cryostat. 3–10 μm frontal cryosections were placed on gelatin-coated slides and stored at −20°C until required for immunostaining within 48 h. Tissue for N-CAM staining was prefixed in 2·5% paraformaldehyde in PBS and then handled as above. Lectins were applied to both prefixed and nonfixed cryosections.

MZ15 was applied to wax sections for greater histological detail. The tissue was fixed in precooled 96% methanol overnight at 4°C, then dehydrated, cleared and embedded in low melting-point paraffin wax according to the method of Sainte-Marie (1962). Blocks were stored at 4°C until required for sectioning. 5–10 μm sections were placed on gelatin-

Table 1. *Binding specificities of lectins and glycosaminoglycans (GAGs) that contain these sugar residues and hence may bind the lectins*

			GAG				
Lectin	Source	Structures recognized	Hyaluronate	Chondroitin sulphate	Dermatan sulphate	Heparan sulphate	Keratan sulphate
ConA	Jackbean *Canavalia ensiformis*	α-D-Glc; α-D-Man	+	−	−	−	−
DBA	*Dolicos biflorus*	α-D-GalNAc	−	−	−	−	−
PNA	Peanut *Arachis hypogea*	β-D-Gal; β-D-GalNAc	−	++	++	+	+++
RCA1	Castor bean *Ricinis communis*	β-D-Gal	−	+	+	+	++
SBA	Soybean *Glycine max*	(α-D-Gal); α/β-D-GalNAc	−	++	++	−	+
UEA1	*Ulex europaeus*	α-L-fuc	+	−	−	−	−
WGA	Wheatgerm *Triticum vulgare*	$(\beta\text{-D-GlcNAc})_2$ sialic acid	++	−	−	−	++

No correspondence between lectin specificity and sugar residues of GAG (−); the lectin binds to a minor sugar residue of the GAG (+); the lectin binds to one of the repeating disaccharides of the GAG (++); and lectin binds to both minor and major sugars of the GAG (+++). Derived from Lis & Sharon, 1977; Alberts *et al.* 1983 and Rittman & Mackenzie, 1983 (scoring ++ for lectin binding to a major sugar component, and + for binding to a minor sugar component of the GAG).

coated slides, allowed to air dry and stored at 4°C prior to staining. Tissue for general histology was fixed overnight in freshly prepared half-strength Karnovsky's fixative at 4°C (Karnovsky, 1965). Specimens were rinsed in 0·1 M-cacodylate buffer, dehydrated and embedded in Araldite resin. 1 μm sections were mounted on glass slides and stained with toluidine blue.

Staining methods

Anti-type-II collagen, anti-HSPG, MZ15 and anti-N-CAM antibodies were applied to cryosections and observed using fluorescein–isothiocyanate (FITC)-conjugated secondary antibodies. The Sainte-Marie-prepared wax sections were stained with MZ15 and visualized with FITC-conjugated secondary antibodies or the peroxidase anti-peroxidase system (PAP, Amersham).

The biotinylated lectins were applied to cryosections (Rittman & Mackenzie, 1983) and observed with the application of a biotin–streptavidin complex conjugated with the red fluorescent phycobiliprotein, Phycoerythrin (PE-SA, Amersham). Lectins are metalloproteins, therefore PBS was replaced with Tris-buffered saline (TBS, 100 mM-Trizma base (Sigma), 100 mM-sodium acetate, pH 7·3) to maintain the correct balance of ions necessary for efficient saccharide binding.

(a) *Cryosections*

Sections were moistened with PBS (N-CAM) or TBS (other) in a humidified air chamber. To prevent masking by other matrix components, sections to be treated with MZ15 or antibodies to collagen type II and HSPG were pretreated with chondroitinase (0·25 i.u. ml^{-1}, Sigma), and Streptomyces hyaluronidase (1·45 i.u. ml^{-1}, Sigma), for 30 min, then washed (PBS/TBS, twice 10 min). Similarly, half of the sections to be stained with lectins were pretreated with neuraminadase to remove sialic acid, in order to assess the extent of masking by such components.

Primary solutions were applied for 45–60 min (anti-type-II collagen 1:20, anti-HSPG hybridoma supernatant 1:1000 and MZ15 1:1000 in TBS/0·1% BSA/0·01% azide; lectins 10 μg ml^{-1} in 10 mM-Hepes, 0·15 M-NaCl, 0·1 mM-Ca^{2+}, 0·04% azide, pH 7·5) or overnight (anti-N-CAM 1:1000 in PBS/0·1% BSA/0·01% azide) then washed (PBS/TBS, twice 10 min).

Secondary solutions were incubated on the sections for 30 min (FITC-conjugated swine anti-rabbit IgG at 1:50 in TBS/0·1% BSA/0·01% azide for anti-type-II collagen; and FITC-conjugated rabbit anti-mouse IgG at 1:50 in TBS/0·1% BSA/0·01% azide for anti-HSPG and MZ15; FITC-conjugated swine anti-rabbit IgG at 1:50 in PBS/0·1% azide for anti-N-CAM; and PE-SA for lectins.

Sections were given a final rinse (PBS/TBS, twice 10 min) and mounted in glycerol/PBS (1:9 v/v), containing DABCO (Sigma), to preserve the fluorescence during subsequent microscopy (Johnson *et al.* 1982). Photographs were taken on a Zeiss photomicroscope with an epifluorescence attachment using HP5 35 mm film (Ilford).

Controls were processed either without the primary solution or with the relevant non-immune serum. The control sections were enzyme pretreated where applicable, for example control sections for lectins were also pretreated with neuraminidase and control sections for MZ15 or collagen type-II were pretreated with chondroitinase and hyaluronidase.

(b) *Paraffin wax sections*

Sections were dewaxed, hydrated and stained as above with MZ15 and with FITC-conjugated secondary antibodies. Controls were as for cryosections.

Results

The staining patterns produced by antibodies to collagen type II, keratan sulphate, N-CAM and the lectin binding in the nasal placodes and passages are summarized in Table 2 and details indicated in Tables 3, 4, 5. The lectin-binding specificities and the glycosaminoglycans that contain these sugar residues are shown in Table 1.

Table 2. *Summary of the staining patterns produced within the definitive chick nasal passages by antibodies and lectins*

Antibody/lectin		10-day old nasal epithelium: Respiratory		Olfactory		Differential staining (suitable markers *)
Antibody						
anti-N-CAM		−		++		*
MZ15 (anti-keratan sulphate)		+/−		+++	(S)	*
anti-collagen type-II		+++	(BMZ)	+++	(BMZ)	
Lectin (on prefixed tissue)	N'ase					
ConA	P/A	+		+++	(S)	*
DBA	P/A	+	(BMZ)	+	(BMZ)	
PNA	P	−		+	(S)	*
PNA	A	++	(BMZ)	++	(BMZ)	
RCA1	P/A	−		+++	(S)	*
SBA	P	−		+++	(S)	*
SBA	A	++	(BMZ)	−		
UEA1	P/A	−		−		
WGA	P/A	−		+++	(S)	*

Extent of staining: strong (+++), moderate (++), weak (+), negligible (+/−), and absent (−). Localization of staining if not throughout epithelium: surface staining (S), basement membrane zone localization (BMZ). N'ase = neuraminidase pretreatment, result obtained in presence of (P), in absence of (A), with or without (P/A) enzyme pretreatment.

Characteristics of epithelial domains within the nasal passages

The binding patterns of several antibodies and lectins distinguish between the olfactory epithelium and respiratory epithelium. Antibodies to N-CAM and keratan sulphate, and the lectins ConA, PNA, RCA1, SBA and WGA all specifically bind to regions of the olfactory epithelium (Table 2). Fig. 1 shows their distribution in the nasal passages of the chick embryo at 10 days of development. The olfactory epithelium covers the superior concha, the roof of the nasal cavity and adjacent nasal septum; and the respiratory epithelium lines the remainder, which includes both the middle and the more distal vestibular conchae.

N-CAM expression is confined to the olfactory epithelium and adjacent olfactory nerve bundles (Fig. 2A,B,E). In comparison, the respiratory epithelium, which covers the middle concha, is negative for N-CAM staining (Fig. 2C,D) and this nonreactivity of the respiratory epithelium is made all the more striking by the expression of N-CAM in the surrounding mesenchyme (Fig. 2C,D). There is an abrupt limit in N-CAM expression corresponding to the histological boundary between the olfactory and respiratory epithelial types.

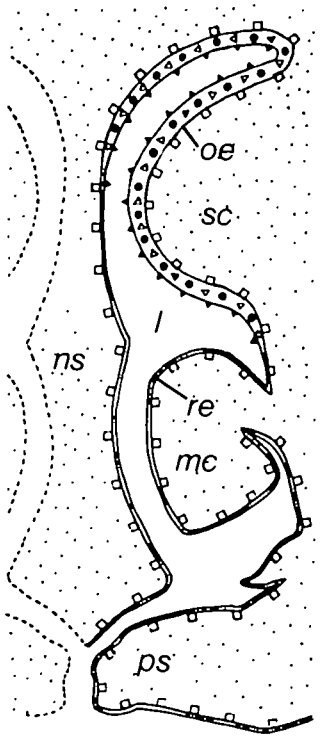

Fig. 1. Diagrammatic summary of the distribution of MZ15, a panel of lectins, N-CAM, Collagen type II and HSPG in stage 35 chick nasal passages (only one cavity is shown). Key: staining pattern produced with: (●) antibodies to N-CAM; (▲) ConA, PNA, RCA1, SBA, WGA and MZ15; (△) MZ15, weak staining only; (□) collagen type II and HSPG. Lumen (l); middle concha (mc); nasal septum (ns); olfactory epithelium (oe); palatal shelf (ps); respiratory epithelium (re); superior concha (sc).

In addition to the striking localization of N-CAM, the lectins ConA, PNA, RCA1, SBA and WGA all bind to the surface of the olfactory epithelium but not to the respiratory epithelium. Fixation enhances the binding of ConA (Fig. 3B *vs.* 3A), RCA1 (Fig. 3E), SBA (Fig. 3G *vs.* 3H) and WGA (Fig. 3F). UEA1 does not bind significantly under any conditions (Fig. 3C,D). The binding of ConA, RCA1 and WGA to the surface of the olfactory epithelium in fixed tissue is irrespective of neuraminidase pretreatment. In contrast, SBA only binds to the olfactory epithelium of fixed tissue that has been enzyme pretreated (Fig. 3H *vs.* 3I).

Lectins not only bind to the cell surface but also bind to the basement membrane zone. Both DBA and RCA1 bind to the basement membrane zone under both the olfactory and respiratory epithelia in unfixed material (Fig. 3E,J), and PNA binds to the basement membrane zones of both olfactory and respiratory epithelia in the absence of neuraminidase pretreatment (Fig. 3K,L,M). RCA1 and PNA are predicted to bind to the sugars present in heparan sulphate (Table 1), and an antibody to heparan sulphate proteoglycan (HSPG) stains the basement membrane zone under both nasal epithelia (not shown).

The olfactory epithelium, which is marked by the binding patterns of PNA, RCA1, SBA and WGA, is also positively stained by the antibody MZ15, which recognizes keratan sulphate. Therefore, these lectins may be recognizing keratan-sulphate-containing proteoglycans (see Table 1) in the olfactory epithelium. MZ15 stains only the thickened olfactory epithelium and its continuation with the lining of the maxillary sinus (Fig. 4D). The respiratory epithelium, lining the middle concha and lower nasal septum, does not significantly stain with MZ15 (Fig. 4D). As the nasal epithelium changes from the thick olfactory epithelium to thinner respiratory epithelium, there is an abrupt decrease in MZ15 staining (Fig. 4E). It is the surface of the olfactory epithelium that exhibits the strongest

Table 3. *Extent and localization of staining for antibodies to collagen type II, keratan sulphate, heparan sulphate proteoglycan (HSPG), and N-CAM during chick nasal development*

	Stage 15–19 placode			Stage 24–25 pit			Stage 27–30 presumptive olfactory			Stage 27–30 epithelium respiratory			Stage 33–36 presumptive olfactory			Stage 33–36 epithelium respiratory		
Antibody	S	E	BMZ	S	E	BMZ	S	E	BMZ	S	E	BMZ	S	E	BMZ	S	E	BMZ
anti-N-CAM	+	++	−	−	++	−							−	++	−	−	−	−
MZ15	+++	++	+++	+++	++	+++	+++	++	++	+++	−	−	+++	++	−	−	−	−
anti-collagen type II	−	−	++	−	−	++	−	−	++	−	−	++	−	−	+	−	−	+
anti-HSPG	−	−	++										−	−	++	−	−	++

Extent of staining: strong (+++), moderate (++), weak (+), negligible (+/−), and absent (−). Localization of staining: surface staining (S), within epithelium (E), basement membrane zone localization (BMZ).

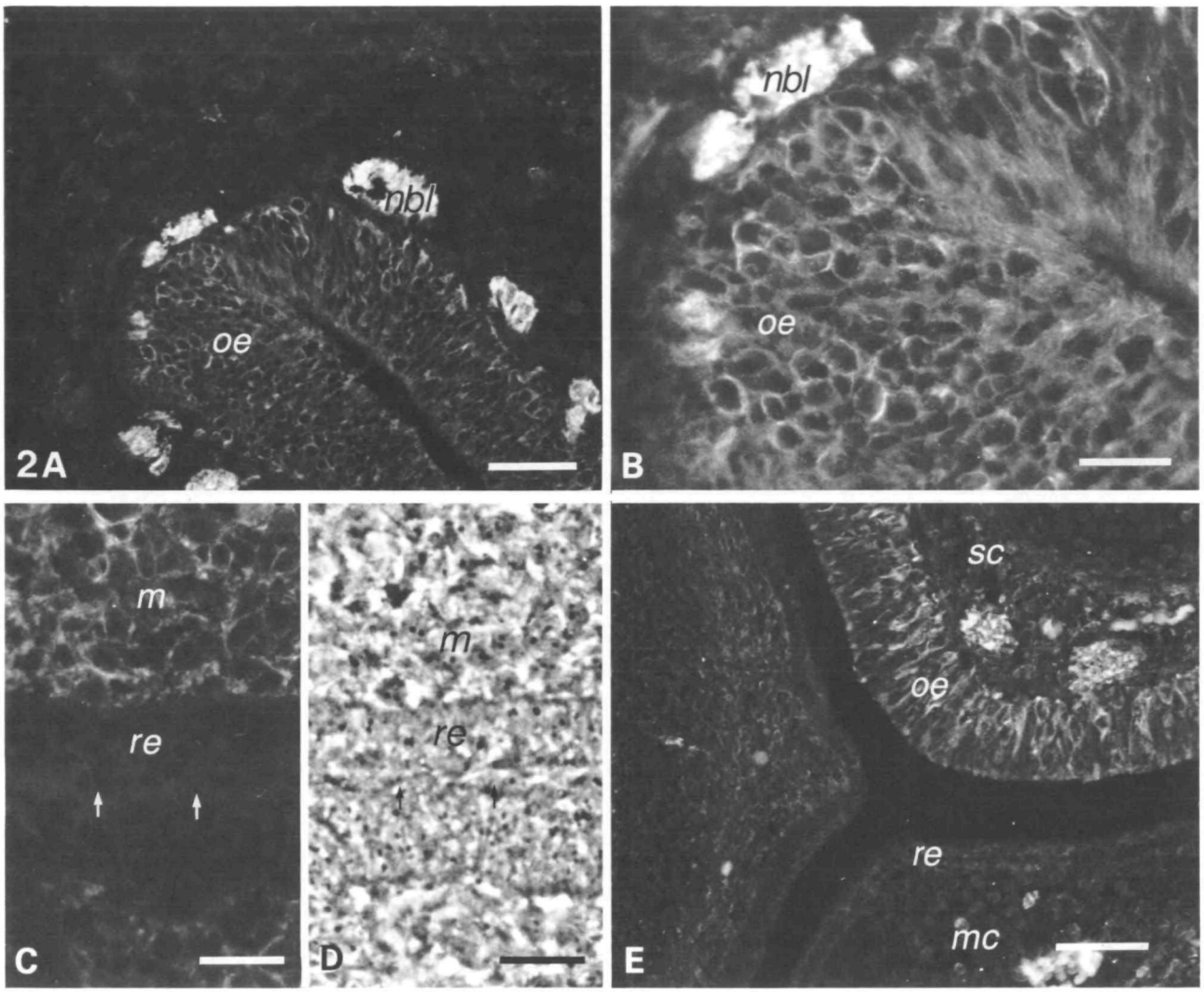

Fig. 2. Distribution of N-CAM in chick nasal epithelia, using 3–4 μm frontal cryosections. Stage 33–36 nasal passage. (A,B) N-CAM is present on cells of the olfactory epithelium (oe), and the underlying olfactory nerve bundles (nbl). Bar, in A, equals 25 μm; and in B, equals 10 μm. (C) Immunofluorescence and (D) matching micrographs of anti-N-CAM staining. N-CAM is absent in the respiratory epithelium (re). The facial mesenchyme (m) exhibits some staining. The slit between the two epithelia runs across the centre of the photograph (arrows). Bar, 10 μm. (E) Section showing epithelia on the two conchae illustrates the striking difference between the positively staining olfactory epithelium (oe) on the superior concha (sc), and the negative respiratory epithelium (re) on the middle concha (mc). Bar, 25 μm.

staining, with weaker staining within the olfactory epithelium itself (Fig. 4D,E). MZ15 also stains the nasal capsule cartilage (Fig. 4E).

Temporal and spatial changes in epithelial characteristics during development

The stages of chick nasal development have been well documented (Bancroft & Bellairs, 1977; Yee & Abbott, 1978; Will & Meller, 1981; Tamarin *et al.* 1984) and are summarized in Fig. 5. The olfactory placodes first become visible after 2–2·5 days of development, as shallow depressions on either side of the presumptive face (Fig. 5A,B). With further development the nasal pits invaginate to form shallow grooves (Fig. 5C,D), with the thickened epithelium becoming localized distally. The nasal cavities become further elaborated by outgrowths, or conchae, from the lateral wall of the nasal passages (Fig. 5E,F,G,H). In the definitive nasal passages, the olfactory epithelium lines the superior concha, the respiratory epithelium covers the middle concha (Fig. 5G,H).

All the markers of olfactory cells are found spread throughout the ectoderm of the placode and surrounding head of the early embryo but become restricted to the olfactory epithelium during development. For example, in the early embryo, stage 15, N-CAM is present in the thickened placodal epithelium and general head ectoderm (Fig. 6A,B), but it is confined to the olfactory epithelium in the mature nasal passage (Fig. 2A,B,E). In the early embryo, N-CAM is also expressed within a cell mass in the mesenchyme immediately beneath the nasal placode (Fig. 6A). This

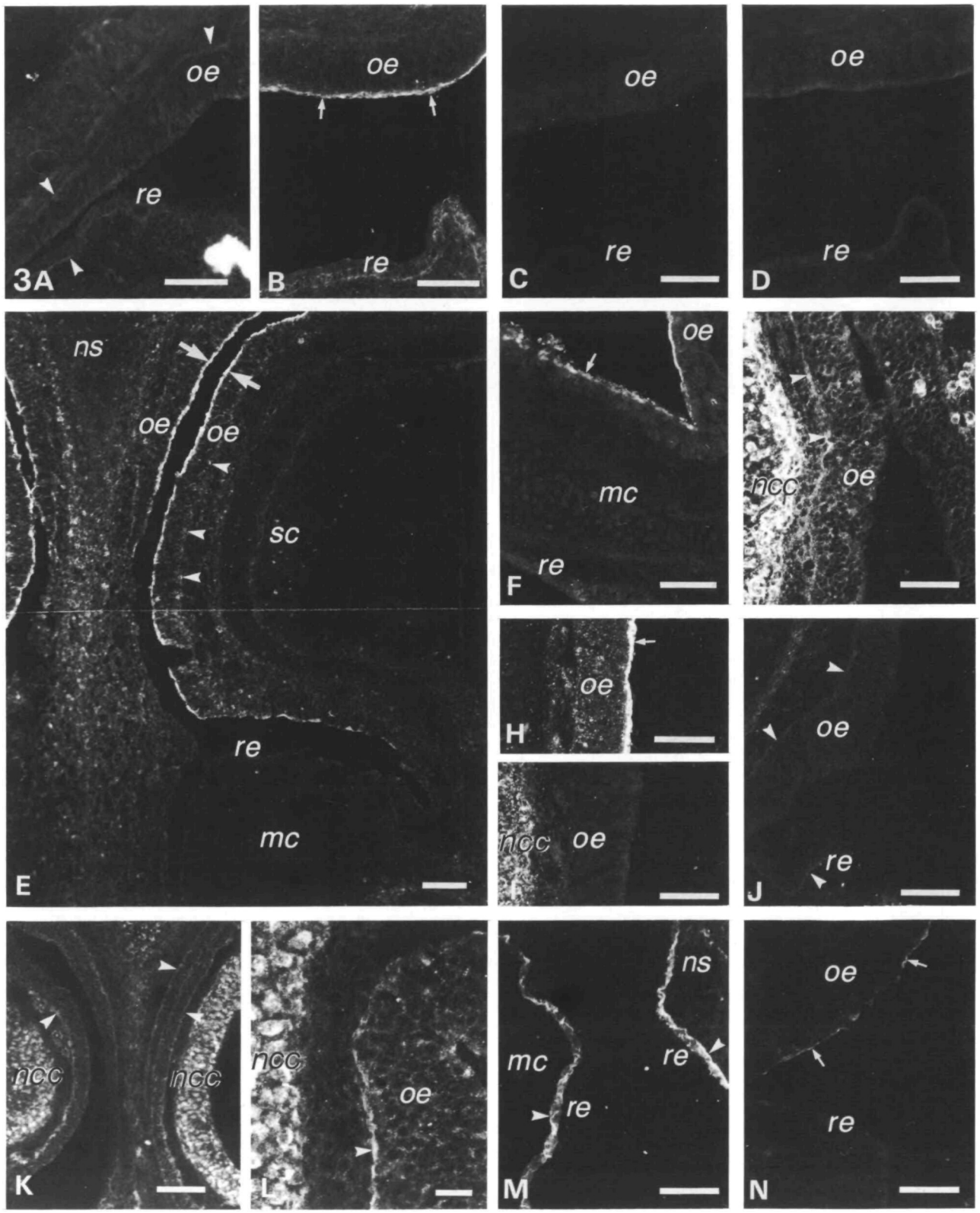

Fig. 3. For legend see p. 500

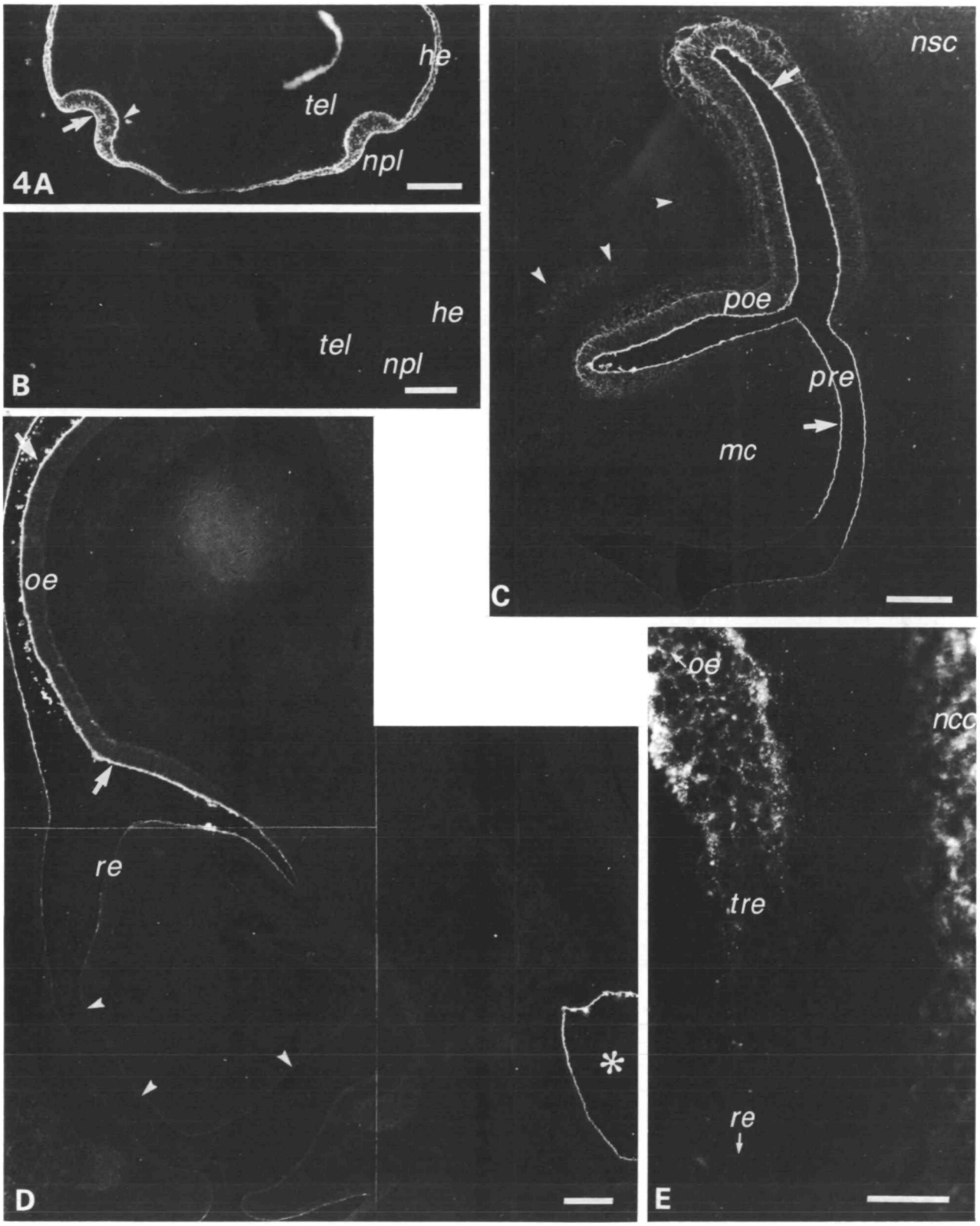

Fig. 4. For legend see p. 500

Fig. 3. Lectin binding to chick nasal epithelia, on prefixed or unfixed frontal cryosections. N'ase = pretreatment of sections with neuraminidase, result obtained with (+), or without (−) enzyme pretreatment. In instances where the conditions of fixation or enzyme pretreatment do not affect the result obtained, the conditions used are given in brackets.

(A) ConA, unfixed (+N'ase). ConA binds weakly to the basement membrane zone (arrowheads) underlying the olfactory epithelium (oe) and respiratory epithelium (re). Bar, 25 μm.

(B) ConA, prefixed (+N'ase). ConA binds intensely to the surface (arrows) of the olfactory epithelium (oe) on the superior concha (sc). There is some binding to the respiratory epithelium (re), but this is less pronounced. Bar, 25 μm.

(C) UEA1, unfixed (+N'ase). UEA1 does not bind to either the olfactory epithelium (oe) or the respiratory epithelium (re). Bar, 25 μm.

(D) UEA1, prefixed (−N'ase). UEA1 still does not bind significantly to the olfactory (oe) or respiratory epithelia (re), even after fixation. Bar, 25 μm.

(E) RCA1, prefixed (−N'ase). There is a striking pattern of RCA1 binding to the surface (arrows) of the olfactory epithelium (oe) on the superior concha (sc) and upper nasal septum (ns). The respiratory epithelium (re) on the middle concha (mc) and lower nasal septum does not bind RCA1. There is weak binding of RCA1 to the basement zone (arrowheads) of the olfactory epithelium. Bar, 50 μm.

(F) WGA, prefixed (−N'ase). WGA binds strongly to the surface of the olfactory epithelium (oe) on the superior concha and to the epithelium (arrow) on the upper surface of the middle concha (mc). The respiratory epithelium (re) on the underside of the middle concha does not bind WGA. Bar, 25 μm.

(G) SBA, unfixed (−N'ase). SBA strongly binds to the cartilage of the nasal capsule (ncc), and to the basement membrane zone (arrowheads) underlying the olfactory epithelium (oe). Bar, 25 μm.

(H) SBA, prefixed, −N'ase. SBA gives intense staining of the olfactory surface (oe, arrows). The basement membrane beneath the epithelium does not bind SBA. Bar, 25 μm.

(I) SBA, prefixed, +N'ase. SBA binds to the nasal capsule cartilage (ncc), but not to the olfactory epithelium itself (oe). Bar, 25 μm.

(J) DBA, unfixed (+N'ase). DBA does not bind to the surface of the olfactory epithelium (oe). There is weak binding of DBA to the basement membrane zone (arrowheads) beneath this epithelium and the respiratory epithelium (re). Bar, 25 μm.

(K) PNA, −N'ase, unfixed. PNA binds strongly to the nasal capsule cartilage (ncc) in unfixed tissue. The basement membrane zone beneath the olfactory epithelium binds PNA (arrowheads). Bar, 50 μm.

(L) PNA, −N'ase, unfixed. Detail of the basement membrane binding of PNA (arrowheads) beneath the olfactory epithelium (oe) and in the nasal capsule cartilage (ncc). Bar, 10 μm.

(M) PNA, −N'ase, unfixed. The basement membrane zone (arrowheads) beneath the respiratory epithelium (re) on the middle concha (mc) and nasal septum (ns) binds PNA more strongly than under the olfactory epithelium. Bar, 25 μm.

(N) PNA, +N'ase (prefixed). PNA binds only to the surface (arrows) of the olfactory epithelium (oe) and not to the respiratory epithelium (re). Bar, 25 μm.

Fig. 4. Distribution of keratan sulphate in chick nasal development (using MZ15 on frontal wax sections, except on frontal cryosections in E).

Stage 17 nasal placodes.

(A) Keratan sulphate is located throughout the head ectoderm (he), including the thickened placodal epithelium (npl). The telencephalon (tel) does not stain. The surface (arrow) and basement membrane zone (arrowhead) of the placodal epithelium exhibit enhanced staining. Bar, 50 μm.

(B) Control section treated with second antibody only is negative. Bar, 50 μm.

Stage 30 nasal passages.

(C) Keratan sulphate is found particularly at the surface (arrows) of the presumptive olfactory epithelium (poe) on the superior concha (sc), and part of the presumptive respiratory epithelium (pre) on the middle concha (mc). The condensing chondrogenic mesenchyme of the nasal septal cartilage (nsc) and nasal capsule cartilage (ncc) exhibit keratan sulphate (arrowheads). Bar, 25 μm.

Stage 36 nasal passage.

(D) Keratan sulphate is present particularly on the surface (arrows) of the olfactory epithelium (oe), and weakly within the epithelium. The respiratory epithelium (re) shows slight staining on the upper middle concha, but the epithelium covering the lower middle concha (arrowheads) does not stain. The lining of the maxillary sinus (*) is also positive. Bar, 50 μm.

(E) Gradual loss of keratan sulphate staining passing from the thickened olfactory epithelium (oe) towards the thinner epithelium in the transitional zone (tre) between the olfactory and respiratory epithelia (re). The nasal capsule cartilage (ncc) also stains. Bar, 10 μm.

cell mass may represent epithelioid cells which are known to migrate out of the nasal placode towards the telencephalon (Robecchi, 1972; Cushieri & Bannister, 1975*a*,*b*; and Mendoza *et al.* 1982). As the nasal placode invaginates to form the nasal pit, stages 24–28, N-CAM staining becomes localized to the deeper regions of the pit within the presumptive olfactory epithelium and is lost from the presumptive respiratory epithelium.

The sugar residues to which the lectins bind are not only present on the olfactory epithelium, but are also found on the nasal placode and head ectoderm (Table 5). The lectins ConA (Fig. 7A,B), DBA (Fig. 7C,D), SBA (Fig. 7E,F), RCA1 (Fig. 7G,H), WGA (Fig. 7J) and PNA (Fig. 7K,L), all bind to the placodal epithelium, particularly at the surface and basement membrane zone, but the lectin UEA1 does not give significant staining of the nasal placode and adjacent head structures at this stage of development (Fig. 7I). Fixation enhances the binding of the lectins ConA (Fig. 7B *vs.* 7A), DBA (Fig. 7D *vs.* 7C), SBA (Fig. 7F *vs.* 7E) and RCA1 (Fig. 7H *vs.* 7G) to the basement membrane zone underlying the placode and adjacent head ectoderm. None of the binding patterns produced by these lectins are significantly altered by

pretreatment of the cryosections with neuraminidase, except for PNA, which has a bold pattern of binding to the basement membrane zone under both the placode and telencephalon (Fig. 7K) and loses this striking localization after neuraminidase pretreatment (Fig. 7L).

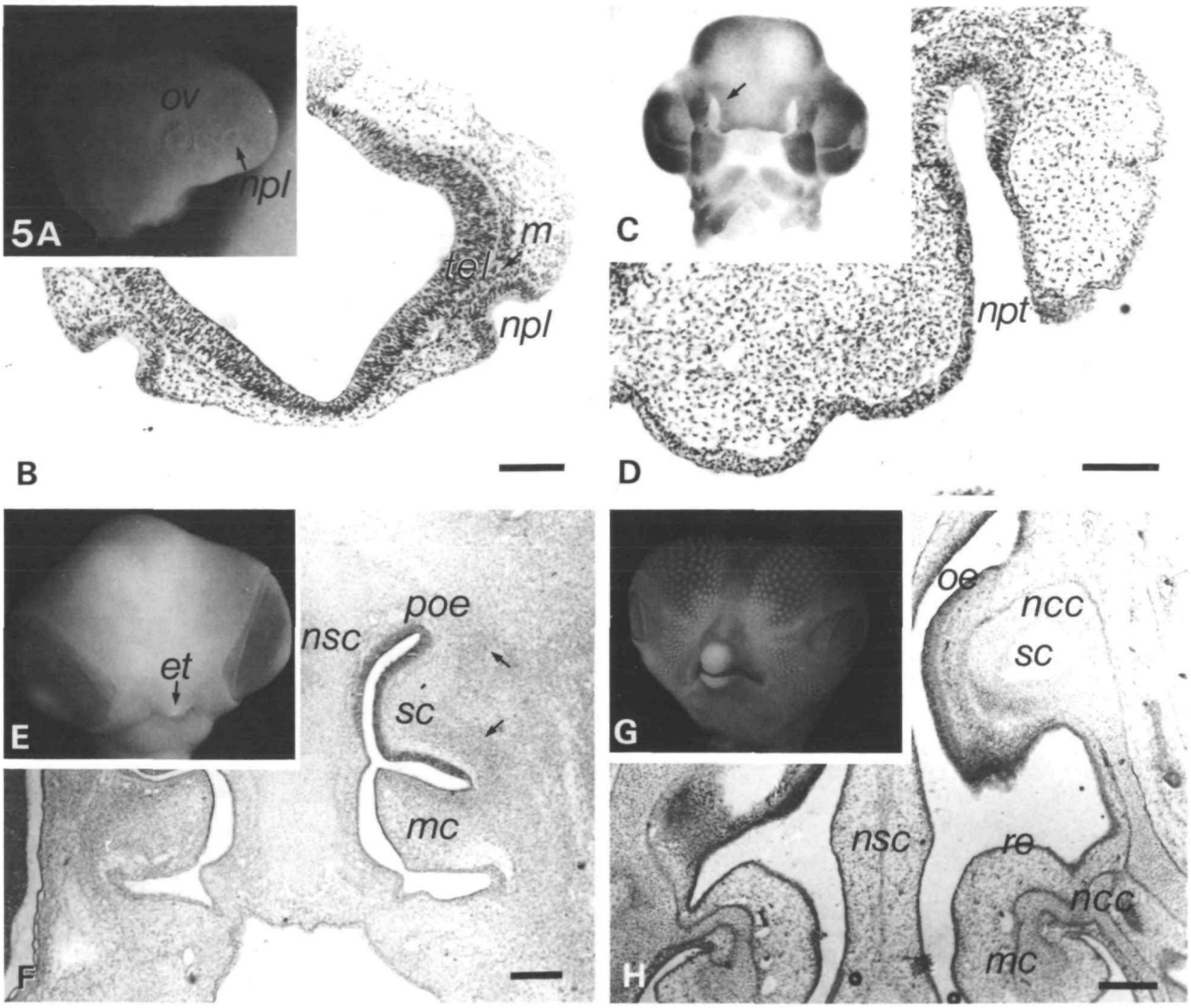

Fig. 5. Stages of nasal development in the chick embryo, illustrated in wholemount and 1 μm frontal Araldite sections stained with toluidine blue.

Stage 17 (2·5 days, 29–32 somites).

(A) Side view of head showing right nasal placode (npl, arrow), and optic vesicle (ov).

(B) Note the close proximity of the base of the placode (npl) to the telencephalon (tel) and thin layer of mesenchyme (m) separating them (arrow). Bar, 50 μm.

Stage 24 (4 days).

(C) The nasal pits are no longer circular, but have elongated (arrow). The facial processes have formed.

(D) The nasal pit (npt) has deepened, with the thickened epithelium (tce) localized distally and to the roof of the nasal cavity. Bar, 50 μm.

Stage 30 (6·5 days).

(E) The upper beak has grown forward between the nostrils. The egg tooth primordium (et) has formed (arrow).

(F) The presumptive olfactory epithelium (poe) is localized the superior concha (sc), roof of the nasal cavity and adjacent septum. The middle concha (mc) is lined with presumptive respiratory epithelium (pre). The mesenchyme of the nasal septum is condensing to form the septal cartilage (nsc). Within the superior concha the nasal capsule is beginning to form (arrows). Bar, 100 μm.

Stage 36 (10 days).

(G) The whole bill protrudes rostrally and so approaches the characteristic adult form.

(H) Section proximal to the vestibular concha, showing middle concha (mc) lined with respiratory epithelium (re), and superior concha (sc) with olfactory epithelium (oe). The middle concha has begun to coil. The cartilaginous nasal capsule (ncc) invests both conchae and is continuous with the nasal septal cartilage (nsc). The maxillary sinus (arrow), lies lateral to the nasal cavity, close to the eyes. Bar, 100 μm.

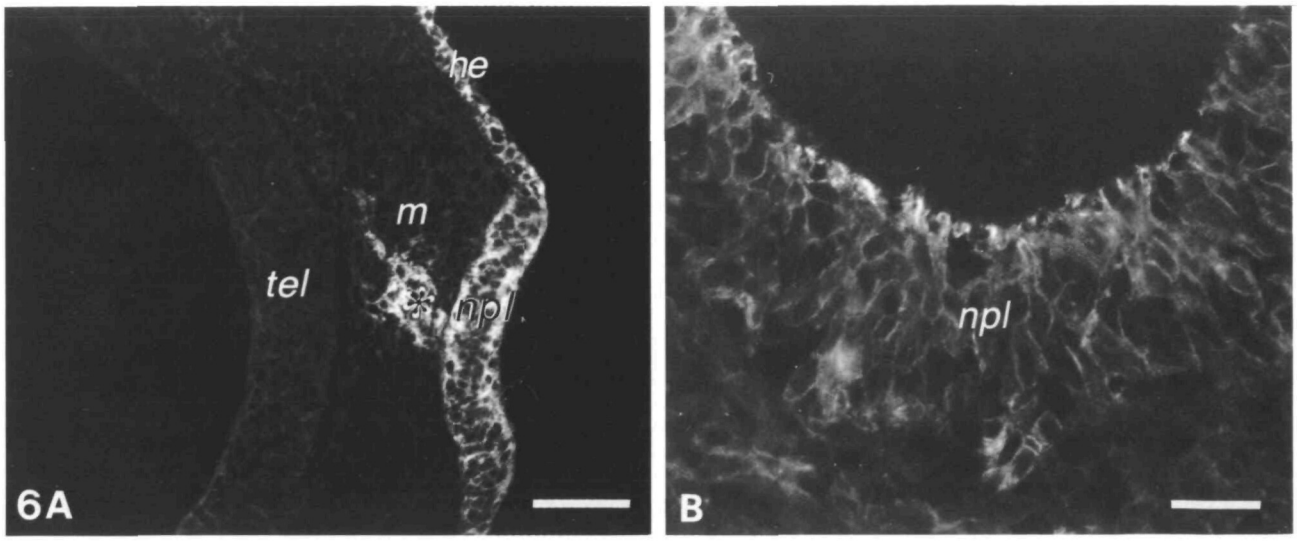

Fig. 6. Expression of N-CAM in the chick nasal placode, on 3–4 μm frontal cryosections.
Stage 15–19 nasal placode.
(A,B) N-CAM is present in the thickened placodal epithelium (npl) and head ectoderm (he). There is virtually no staining in the telencephalon (tel) and mesenchyme (m), except in a mass immediately below the placode (*). Bar, in A, equals 25 μm; and in B, equals 10 μm.

The lectins PNA, RCA1, SBA and WGA bind to sugars contained in keratan sulphate proteoglycan (Table 1). Consistent with the lectin-binding patterns, keratan sulphate is present from the earliest stages of nasal development during placode formation. At stage 17, keratan sulphate is present in the placode and head ectoderm, particularly at the surface and basement membrane zone (Fig. 4A,B). During subsequent development, the presumptive olfactory epithelium becomes localized to the upper and deeper regions of the nasal cavities, and keratan sulphate staining becomes progressively restricted to this thickened sensory epithelium (Fig. 4C). First, there remains some surface staining over the middle concha, which is lined by respiratory epithelium (Fig. 4C), but no staining is present within this epithelium itself. Keratan sulphate, at this stage, is also detected in the cartilage of the nasal septum (Fig. 4C, arrows). Then keratan sulphate is further restricted to the surface of the olfactory epithelium only and the respiratory epithelium does not exhibit significant MZ15 staining (Fig. 4D). Keratan sulphate is distributed particularly along the surface of the olfactory epithelium (Fig. 4A), but there is also some staining within the epithelium itself. In the stage 17 embryo, anti-HSPG stains only the basement membrane zone of the general head ectoderm, placode and telencephalon (not shown).

Comparison of collagen type II and keratan sulphate expression during nasal development

Collagen type II is present at the epithelial–mesenchymal interface of the nasal placode and continues to be expressed throughout nasal development up to the time when overt chondrogenesis takes place within the perinasal mesenchyme. Therefore there is no regional-specific pattern of collagen type II expression within the chick nasal passages. Collagen type II can be detected beneath the nasal placode (Fig. 8A), nasal pit (Fig. 8B), and whole nasal cavity (Fig. 8C,D,E,F). In the early embryo, stage 17, there is also positive staining of type-II collagen at the base of both the general head ectoderm (Fig. 8A), and telencephalon. This contrasts with the expression of keratan sulphate at the epithelial–mesenchymal interface, which, although pronounced at early stages can only be detected in olfactory regions later in development (Fig. 4D,E).

Discussion

This survey of extracellular matrix and cell surface molecules has identified a number of markers for the domains of olfactory epithelium in the chick nasal passages. Antibodies to N-CAM and keratan sulphate, plus a number of lectins all bind to parts of the olfactory epithelium but not to the respiratory epithelial domain, and their binding abruptly stops at the boundary between these two epithelial cell types. The olfactory markers are present in the nasal placode and become progressively restricted to the olfactory domain as development proceeds. A comparison of the distribution of keratan sulphate and collagen type II shows that there is colocalization at early stages in nasal development but unlike keratan sulphate, collagen type II is not restricted to the olfactory domain at later stages of development.

Epithelial domains in the nasal passages

The olfactory epithelial domain of the nasal lining can be distinguished from the respiratory domain by the binding patterns of a number of antibodies and lectins.

Table 4. *Extent and localization of lectin binding to chick nasal epithelia, stage 33–36*

	Unfixed												Fixed											
	olfactory epithelium						respiratory epithelium						olfactory epithelium						respiratory epithelium					
	−N'ase			+N'ase			−N'ase			+N'ase			−N'ase			+N'ase			−N'ase			+N'ase		
Lectin	S	E	BMZ	S	E	BMZ	S	E	BMZ	S	E	BMZ	S	E	BMZ	S	E	BMZ	S	E	BMZ	S	E	BMZ
ConA	++	++	++	−	−	−	++	++	+++	−	−	+	+++	++	++	++	−	−	++	++	+++	−	−	+
DBA	−	−	+	−	−	+	−	−	+	−	−	+	−	−	−	−	−	−	−	−	−	−	−	−
PNA	+	+/−	++	++	−	−	−	−	+++	−	−	−	−	−	+	++	−	−	−	−	++	−	−	−
RCA1	++	++	++	++	++	++	++	++	++	++	++	++	+++	−	−	+	−	−	−	−	−	+	−	−
SBA	−	−	+	−	−	−	−	−	+	−	−	−	−	−	−	+++	−	−	−	−	+	−	−	−
UEA1	−	−	−	−	−	−	−	−	−	−	−	−	−	−	−	−	−	−	−	−	−	−	−	−
WGA	−	−	−	−	−	−	−	−	+	−	−	−	+++	−	−	++	−	−	−	−	−	−	−	−

Extent of staining: strong (+++), moderate (++), weak (+), and absent (−). Localization of staining: surface staining (S), within the epithelium (E), basement membrane zone localization (BMZ). N'ase = pretreatment with neuraminidase, result obtained with (+), without (−) enzyme pretreatment.

Table 5. *Extent and localization of lectin binding to the chick nasal placode, stages 15–19*

	Unfixed												Fixed											
	placode						head ectoderm						placode						head ectoderm					
	−N'ase			+N'ase			−N'ase			+N'ase			−N'ase			+N'ase			−N'ase			+N'ase		
Lectin	S	E	BMZ	S	E	BMZ	S	E	BMZ	S	E	BMZ	S	E	BMZ	S	E	BMZ	S	E	BMZ	S	E	BMZ
ConA	+	+	−				+	+	+				+	−	+	+	−	+	+	−	+	+	−	+
DBA	−	−	−				−	−	−				−	−	+	−	−	+/−	−	−	+	−	−	+
PNA	+	+/−	+++				−	+/−	+++				−	+	+++	+	−	−	−	+	++	+	−	−
RCA1	+	−	−				+	+	++				+	−	−	+++	+	+	+	−	−	++	+	+
SBA	+	+	++				−	−	+				++	++	++	++	+	+	+	++	−	++	−	−
UEA1	−	−	−				−	−	−				−	−	−	−	−	−	−	−	−	−	−	−
WGA	+	−	+/−				+	+	+				+	−	−	+	−	−	+	+	−	+	−	−

Extent of staining: strong (+++), moderate (++), weak (+), and absent (−). Localization of staining: surface staining (S), within the epithelium (E), basement membrane zone staining (BMZ). N'ase = pretreatment with neuraminidase, result obtained with (+), without (−) enzyme pretreatment.

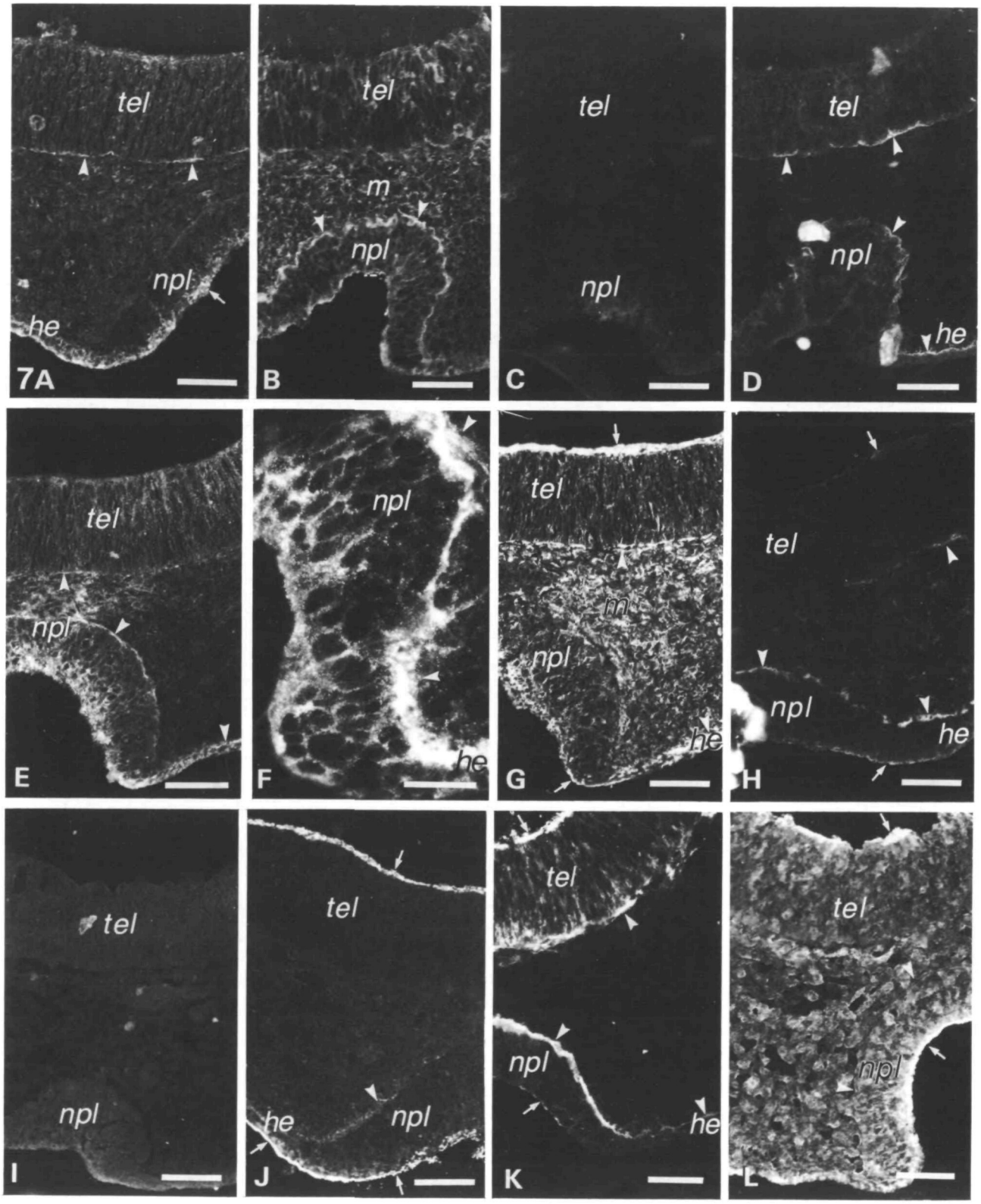

Antibodies to N-CAM and keratan sulphate, plus the lectins ConA, PNA, RCA1, SBA and WGA all characterize the olfactory domain. There is an abrupt change in epithelial character, as recognized by these antibodies and lectins, at the junction between olfactory and respiratory epithelia. The localization of N-CAM expression to the sensory olfactory epithelium of the nasal lining shows a striking similarity to the regionalization of N-CAM (Richardson *et al.* 1987) and A-CAM (Raphael *et al.* 1988) in the developing ear. In the ear,

Fig. 7. Lectin binding to the chick nasal placode, on prefixed and unfixed frontal cryosections. N'ase = pretreatment of sections with neuraminidase, result obtained with (+) or without (−) enzyme pretreatment. In instances where the conditions of fixation or enzyme pretreatment do not affect the result obtained, the conditions used are given in brackets.

Stage 17 nasal placode.

(A) ConA, unfixed (−N'ase). ConA, like RCA1, SBA and WGA binds to the nasal placode (npl), particularly at the epithelial surface (arrow). The general head ectoderm (he) also stains. The basement membrane zone underneath the telencephalon (tel) binds ConA (arrowheads). Bar, 25 μm.

(B) ConA, prefixed (−N'ase). ConA binds strongly to the epithelial–mesenchymal interface (arrowheads) of the nasal placode (npl). There is also weak staining of the mesenchyme (m). The telencephalon (tel) does not bind ConA. Bar, 25 μm.

(C) DBA, unfixed (−N'ase). DBA does not bind to the nasal placode (npl) or adjacent tissues. Bar, 25 μm.

(D) DBA, prefixed (−N'ase). DBA binds to the basement membrane zone (arrowheads) of the nasal placode (npl), head ectoderm (he) and telencephalon (tel). Bar, 25 μm.

(E) SBA, −N'ase (unfixed). SBA binds to the nasal placode epithelium (npl), and to the basement membrane zone underlying the placode (arrowheads). Bar, 25 μm.

(F) SBA, +N'ase (prefixed). SBA shows strong binding to the basement zone (arrowheads) and throughout both the nasal placode (npl) and head ectoderm (he). Bar, 25 μm.

(G) RCA1, −N'ase (unfixed). RCA1 binds to the surface (arrows) and basement membrane zone (arrowheads) of the nasal placode (npl), head ectoderm (he) and telencephalon (tel). The mesenchyme (m) also binds RCA1. Bar, 25 μm.

(H) RCA1, +N'ase (prefixed). RCA1 binds to the surface (arrows) and basement membrane zone (arrowheads) of the nasal placode (npl), head ectoderm (he), and telencephalon (tel). Bar, 25 μm.

(I) UEA1 (−N'ase, prefixed). There is negligible binding of UEA1 to the nasal placode (npl) and adjacent tissues. Bar, 25 μm.

(J) WGA, unfixed (−N'ase). WGA binds to the surface (arrows) of the head ectoderm (he), placode (npl) and telencephalon (tel). There is weak binding of WGA to the epithelial–mesenchymal interface of the placode (arrowheads). Bar, 25 μm.

(K) PNA, −N'ase (prefixed). PNA binds strongly to the epithelial–mesenchymal interface (arrowheads) of the nasal placode (npl), head ectoderm (he) and telencephalon (tel). There is weak surface binding to the placode and considerable binding to the telencephalon (arrows). Bar, 25 μm.

(L) PNA, +N'ase (prefixed). Enzyme pretreatment removes the binding of PNA to the basement-membrane zone (arrowheads) of the placode (npl)(compare with Fig. 8K). The binding of PNA to the surface (arrows) of the placode and telencephalon (tel) remains. Bar, 25 μm.

the expression of N-CAM becomes localized to the ventral regions of the otocyst and invests only the sensory regions. The striking boundary in N-CAM expression at the junction between two distinct domains in both nasal and aural epithelia supports the idea that N-CAM may be involved in the production and maintenance of boundaries between histologically and functionally distinct cell types within an epithelium. The maintenance of such boundaries is of particular importance since human tumours, for example in the cervix, appear to arise at junctions between distinct epithelial domains (Richart, 1966).

In addition to the restriction of N-CAM expression to the olfactory epithelial domain, MZ15, an antibody to keratan sulphate also shows restricted binding to the olfactory epithelial domain of the nasal lining. The pattern of lectin binding shows that the olfactory domain is recognized by ConA, PNA, RCA1, SBA and WGA. From their binding specificities (Table 1), all of these lectins except ConA are predicted to recognize some of the sugar components that are contained in the glycosaminoglycan (GAG) keratan sulphate. Therefore, this could provide an explanation for the similarity of the binding patterns of PNA, RCA1, SBA and WGA compared with the antibody MZ15. However, because of the binding affinities of PNA and RCA1, we cannot discount the possibility that chondroitin and dermatan sulphates are also present. ConA, which is not predicted to recognize keratan sulphate, also binds specifically to the olfactory domain. ConA is predicted to bind to hyaluronate and the binding of WGA, which also recognizes sugars present in hyaluronate, is consistent with the presence of hyaluronate in the olfactory domain.

Previous investigations have shown that the olfactory epithelium in *Xenopus* specifically binds SBA, whereas PNA and WGA bind to all neurones of the central nervous system (Key & Giorgi, 1986*a*). In the adult rat and mouse, the olfactory epithelium has been shown to specifically bind ConA, PNA and SBA (Hempstead & Morgan, 1983; Key & Giorgi, 1986*b*). ConA binds particularly to the central layer of the olfactory epithelium (Rat: Hempstead & Morgan, 1983; Frog: Chen *et al.* 1986), which corresponds to the olfactory cells themselves. Here, ConA binds only to the surface epithelial cells of the olfactory domain although the reason for this difference in the embryo is not clear.

Tracing changes in epithelial characteristics to understand the origin of domains in the nasal passages

The development of the olfactory-specific characteristics during morphogenesis of the nasal placode may give clues to the origin of this domain. The reagents anti-N-CAM, MZ15 and ConA, PNA, RCA1, SBA and WGA all characterize the olfactory epithelium in the definitive nasal passages. When we investigated how their distribution changes during development, we found that all of these reagents bind to the nasal placode and then become progressively restricted to the olfactory domain. This pattern is consistent with the idea that the olfactory placode gives rise to the olfactory domain of the epithelium of the nasal passages. If this is the case, what is the origin of the respiratory epithelium? One possibility is that the respiratory epithelium is derived from the adjacent head ectoderm

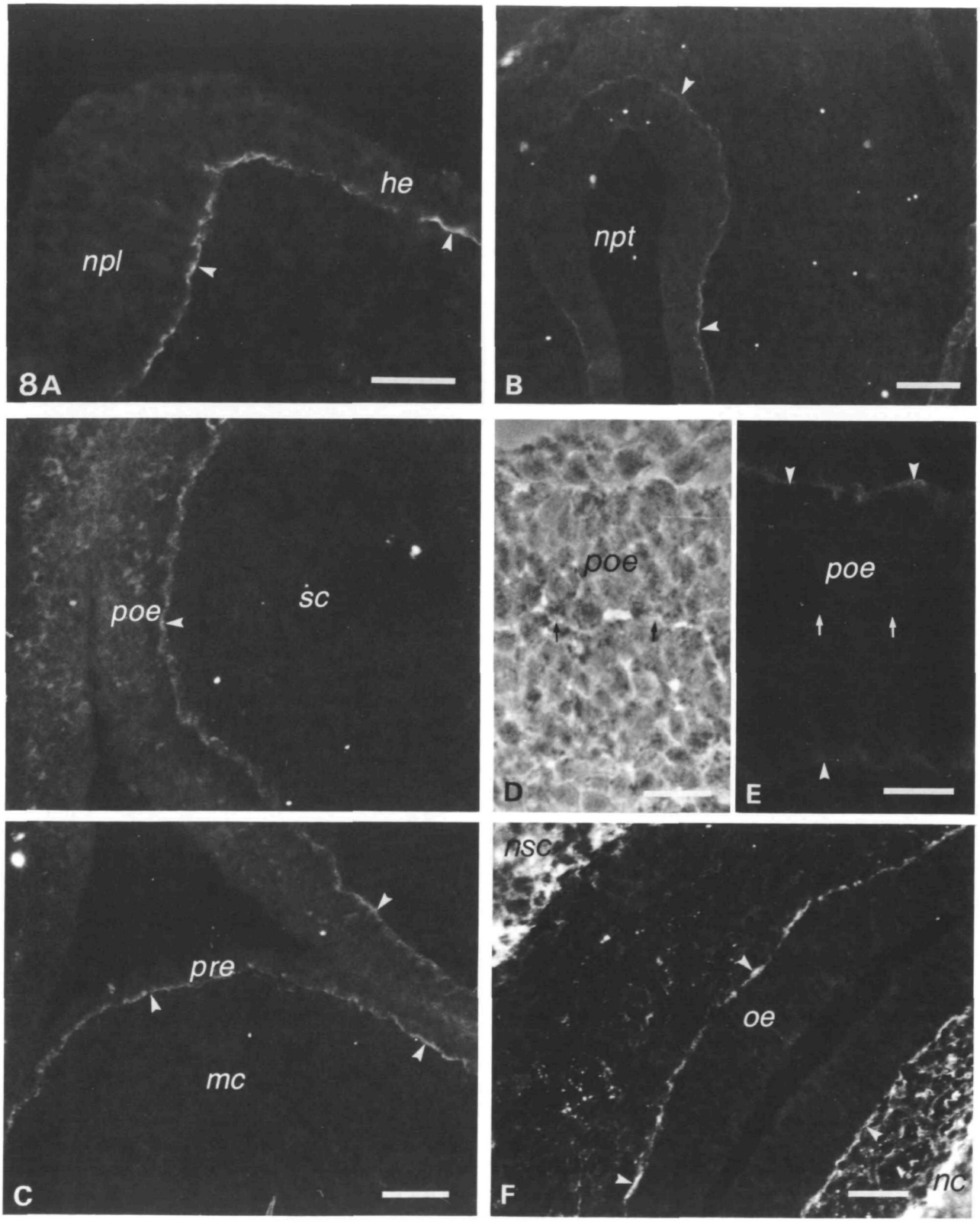

(Street, 1937; Romanoff, 1962). According to this idea, the ectoderm would be drawn into the developing nasal pits as the facial processes enlarge. However, the head ectoderm also binds anti-N-CAM, MZ15 and all of the lectins investigated except UEA1, and yet the respiratory epithelium which develops later is essentially negative for all of these reagents. Therefore, the characteristic patterns of antibody staining and lectin binding do not appear to be cell autonomous and cannot be used to trace the origin of cells. Instead, the changes in the

Fig. 8. Distribution of collagen type II in chick nasal development, using anti-collagen type II antibodies applied to frontal cryosections.

Stage 17 nasal placode.

(A) Collagen type II is found at the epithelial–mesenchymal interface (arrowheads) of the nasal placode (npl) and the general head ectoderm (he). Bar, 10 μm.

Stage 24 nasal pit.

(B) Collagen type II is present in the basement membrane zone (arrowheads) along the whole length of the nasal pit (npt). Bar, 25 μm.

Stage 28–30 nasal passage.

(C) Collagen type II is still present at the epithelial–mesenchymal interface (arrowheads) of both the presumptive olfactory area (poe) on the superior concha (sc), and also in the presumptive respiratory region (pre) on the middle concha (mc). Bar, 25 μm.

(D) Phase-contrast and (E) matching immunofluorescence micrographs of stage 28 presumptive olfactory epithelium (poe) showing localization of collagen type II at the epithelial–mesenchymal interface (arrowheads). The lumen of the nasal passage is represented by a slit (arrows). Bar, in D,E equals 10 μm.

Stage 36 olfactory epithelium.

(F) Collagen type II staining basal to the olfactory epithelium (oe, arrowheads). The cartilages of the nasal septum (nsc) and nasal capsule (ncc) also exhibit collagen type II. Bar, 25 μm.

expression of cell surface characteristics appear to be the result of modulation of expression during development. To further investigate the origins of these epithelial domains we require markers for the respiratory epithelium.

Functional significance of cell surface changes during nasal morphogenesis

Cell surface characteristics may be important in maintaining epithelial shape during folding of the nasal epithelia. It is striking that N-CAM and the cell surface glycoconjugates recognized by specific lectins are present in the early nasal placode and, only after extensive morphogenesis, become restricted to the olfactory epithelium. In mammalian nasal development, it has been found that the lectin ConA binds to the nasal placode, and later particularly to the prospective fusion zones of the nasal folds (Gaare & Langman, 1977; Smuts, 1977 and Burk *et al.* 1979). However, the distribution of the cell surface glycoconjugates found here suggests that they are not solely involved in regions of epithelial fusion and must play some other role.

Extracellular matrix components at the epithelial–mesenchymal interface of the developing nasal epithelium and chondrogenic patterning in the head

The spatial and temporal expression of cartilage-specific extracellular matrix components described here are relevant to the 'Fly-paper model' (Thorogood *et al.* 1986; Thorogood, 1988), which proposes that cranial epithelia (the brain and head ectoderm) act as templates to specify the patterning of chondrogenic differentiation of the neural crest. According to this model, the transient expression of cartilage-specific molecules, in particular collagen type II, at the epithelial–mesenchymal interface acts as an autocatalytic signal to define where neural crest cells will arrest and subsequently differentiate into cartilage.

The distribution of collagen type II correlates spatially with the developing olfactory capsule. Collagen type II can be detected beneath both the olfactory placode and head ectoderm of the early embryo and continues to be associated with the nasal epithelium during development. Such a distribution of collagen type II beneath the chick nasal pit has recently been confirmed (Fitch *et al.* 1989). At later stages, collagen type II is found in the basement membrane zone throughout the nasal passages and therefore is associated with both the olfactory and respiratory epithelia. This spatial distribution correlates with the differentiation of the nasal capsule cartilage, which forms a discrete band that follows the contours of the nasal epithelia. The presence of collagen type II at epithelial–mesenchymal interface of the developing nose is in agreement with its proposed action as a signal that triggers cartilage differentiation to form the nasal capsule, although the timing and duration of specification of perinasal cartilage differentiation is not known.

During chondrogenesis, cartilage-specific matrix components are coordinately expressed (Von der Mark *et al.* 1976; Oettinger *et al.* 1985, and Smith & Watt, 1985). Keratan sulphate is a GAG that is present in both cartilage-specific and noncartilage-specific proteoglycans. The monoclonal antibody, MZ15, recognizes keratan sulphate (Smith & Watt, 1985; Zanetti *et al.* 1985; Mehmet *et al.* 1986). In the chick otic vesicle, there is some degree of colocalization of staining with MZ15 and cartilage-specific collagen type II (Thorogood, 1988; Heath & Thorogood, 1989). Here we have found that in the developing nasal system keratan sulphate does not strictly colocalize with collagen type II. Since the MZ15 antibody recognizes keratan sulphate both in cartilage- and noncartilage-specific proteoglycans, the distribution of keratan sulphate can only be suggestive. For example, the MZ15-positive cell-associated staining probably represents noncartilage-specific proteoglycans (see also Heath & Thorogood, 1989); however, the extracellular staining probably represents cartilage-specific proteoglycans. Therefore, the colocalization of staining with MZ15 and collagen type II antibodies at the interface between the olfactory placode and underlying mesenchyme during early nasal development suggests that cartilage-specific molecules are coordinately expressed at this stage. However, as development proceeds, collagen type II is found beneath the respiratory epithelium, whereas keratan sulphate is absent here. Therefore, it seems unlikely that coordinate expression of these cartilage-specific molecules is required to signal the formation of the nasal capsule cartilage.

Conclusions

The results provide us with several markers to distinguish between respiratory and olfactory epithelial domains in the chick embryo. Antibodies to N-CAM

and keratan sulphate, and the lectins ConA, PNA, RCA1, SBA and WGA specifically bind to the olfactory epithelium. Studies on the expression of a range of intermediate filament proteins have identified markers for the respiratory epithelial domain of the nasal lining (Croucher & Lane, unpublished data). We intend to use these markers to explore the mechanisms that determine epithelial patterning during development.

We wish to thank Dr Tony Leathem (Histopathology, The Middlesex Hospital) for advice on the use of lectins for histochemistry; Professor Lewis Wolpert and Dr Jim Ralphs for reading and commenting on the manuscript. We are indebted to Dr Mark Noble for his help and advice in the preparation of the manuscript. We also thank Lindsay Heath and Dr Peter Thorogood for sending us a copy of their manuscript. S.J.C. is supported by a Medical Research Council Studentship, and the MRC also funds the research of C.T.

References

ALBERTS, B., BRAY, D., LEWIS, J., RAFF, M., ROBERTS, K. & WATSON, J. (1983). The extracellular matrix. In *Molecular Biology of the Cell*, chapter 12, pp. 692–715. Garland.

BANCROFT, M. & BELLAIRS, R. (1977). Placodes of the chick embryo studied by SEM. *Anat. Embryol.* **151**, 97–108.

BAYNE, E. K., ANDERSON, M. J. & FAMBOROUGH, D. M. (1984). Extracellular matrix organization in developing muscle: correlation with acetylcholine receptor aggregates. *J. Cell Biol.* **99**, 1486–1501.

BURK, D., SADLER, T. W. & LANGMAN, J. (1979). Distribution of surface coat material on nasal folds of mouse embryos as demonstrated by Concanavalin A binding. *Anat. Rec.* **193**, 185–196.

CHEN, Z., OPHIR, D. & LANCET, D. (1986). Monoclonal antibodies to ciliary glycoproteins of frog olfactory neurons. *Brain Res.* **368**, 329–338.

CHUONG, C-M. & EDELMAN, G. M. (1984). Alterations in neural cell adhesion molecules during development of different regions of the nervous system. *J. Neurosci.* **4** (9), 2354–2368.

CUSHIERI, A. & BANNISTER, L. H. (1975*a*). The development of the olfactory mucosa in the mouse: light microscopy. *J. Anat.* **119**, 277–286.

CUSHIERI, A. & BANNISTER, L. H. (1975*b*). The development of the olfactory epithelium in the mouse: electron microscopy. *J. Anat.* **119**, 471–498.

EDELMAN, G. M. (1985). Cell adhesion and the molecular processes of morphogenesis. *A. Rev. Biochem.* **54**, 135–169.

FITCH, J. M., MENTZER, A., MAYNE, R. & LINSENMAYER, T. F. (1989). Independent deposition of collagen types II and IX at epithelial-mesenchymal interfaces. *Development* **105**, 85–95.

GAARE, J. D. & LANGMAN, J. (1977). Fusion of nasal swelling in the mouse embryo: surface coat and initial contact. *Am. J. Anat.* **150**, 461–476.

GALLAGHER, B. C. (1986). Basal laminar thinning in branching morphogenesis of the chick lung as demonstrated by lectin probes. *J. Embryol. exp. Morph.* **94**, 173–188.

HAMBURGER, V. & HAMILTON, H. L. (1951). A series of normal stages in the development of the chick embryo. *J. Morph.* **88**, 49–92.

HEATH, L. & THOROGOOD, P. (1989). Keratan sulfate expression during avian craniofacial morphogenesis. *W. Roux Arch. devl Biol.* (in press).

HEMPSTEAD, J. L. & MORGAN, J. I. (1983). Fluorescent lectins as cell-specific markers for the rat olfactory epithelium. *Chemical Senses* **8** (1), 107–120.

JOHNSON, G. D., DAVIDSON, R. S., MCNAMEE, K. C., RUSSELL, G., GOODWIN, D. & HALBAROW, E. J. (1982). Fading of immunofluorescence during microscopy: A study of the phenomenon and its remedy. *J. Immunol. Methods* **55**, 231–242.

KARNOVSKY, M. J. (1965). A formaldehyde gluteraldehyde fixative of high osmolarity for use in electron microscopy. *J. Cell Biol.* **27**, 137.

KEY, B. & GIORGI, P. P. (1986*a*). Selective binding of soybean agglutinin to the surface of the olfactory system in *Xenopus*. *Neuroscience* **18** (2), 507–515.

KEY, B. & GIORGI, P. P. (1986*b*). Soybean agglutinin binding to the olfactory systems of the rat and mouse. *Neurosci. Letts* **69**, 131–136.

LIS, H. & SHARON, N. (1973). The biochemistry of plant lectins (phytohemagglutinins). *A. Rev. Biochem.* **42**, 541–574.

LIS, H. & SHARON, N. (1977). Lectins: Their chemistry and application to immunology. In *'The antigens'* vol. IV, (M. Sela ed.), chapter 7. Academic Press.

MEHMET, H., SCUDDER, P., TANG, P. W., HOUNSELL, E. F., CATERSON, B. & FEIZI, T. (1986). The antigenic determinants recognized by three monoclonal antibodies to keratan sulphate involve sulphated hepta- or larger oligosaccharides of the poly(N-acetyllactosamine) series. *Eur. J. Biochem.* **157**, 385–391.

MENDOZA, A. S., BREIPOHL, W. & MIRAGALL, F. (1982). Cell migration from the chick olfactory placode: a light and electron microscopic study. *J. Embryol. exp. Morph.* **69**, 47–59.

MIRAGALL, F., KADMON, G., HUSMANN, M. & SCHACHNER, M. (1988). Expression of cell adhesion molecules in the olfactory system of the adult mouse: presence of the embryonic form of N-CAM. *Devl Biol.* **129**, 516–531.

OETTINGER, H. F., THAL, G., SASSE, J., HOLTZER, H. & PACIFICO, M. (1985). Immunological analysis of chick notochordal and cartilage matrix development with antisera to cartilage matrix macromolecules. *Devl Biol.* **109**, 63–71.

RAPHAEL, Y., VOLK, T., CROSSIN, K. L., EDELMAN, G. M. & GEIGER, B. (1988). The modulation of cell adhesion molecule expression and intercellular junction formation in the developing avian inner ear. *Devl Biol.* **128**, 222–235.

RICHARDSON, G. P., CROSSIN, K. L., CHUONG, C-M. & EDELMAN, G. M. (1987). Expression of cell adhesion molecules during embryonic induction. III. Development of the otic placode. *Devl Biol.* **119**, 217–230.

RICHART, R. M. (1966). Colpomicroscopic studies of cervical intraepithelial neoplasia. *Cancer* **19**, 395–405.

RITTMAN, B. R. & MACKENZIE, I. C. (1983). Effects of histological processing on lectin binding patterns in oral mucosa and skin. *Histochemical Journal* **15**, 467–474.

ROBECCHI, M. G. (1972). Ultrastructure of differentiation sensory neurons in the olfactory placode of the chick embryo, *Minerva Otolaringologica* **22**, 196–204.

ROMANOFF, A. L. (1960). *The Avian Embryo. Structural and Functional Development.* The Macmillan Company. New York.

SAINTE-MARIE, G. (1962). A paraffin embedding technique for studies employing immunofluorescence. *J. Histochem. Cytochem.* **10**, 250–256.

SMITH, J. C. & WATT, F. M. (1985). Biochemical specificity of *Xenopus* notochord. *Differentiation* **29**, 109–115.

SMUTS, M. S. (1977). Concanavalin A binding to the epithelial surface of the developing mouse olfactory placode. *Anat. Rec.* **188**, 29–38.

STREET, S. F. (1937). The differentiation of the nasal area of the chick embryo in grafts. *J. exp. Zool.* **77**, 49–85.

TAMARIN, A., CRAWLEY, A., LEE, J. & TICKLE, C. (1984). Analysis of upper beak defects in chicken embryos following treatment with retinoic acid. *J. Embryol. exp. Morph.* **84**, 105–123.

THOROGOOD, P. (1988). The developmental specification of the vertebrate skull. *Development* **103 supplement**, 141–153.

THOROGOOD, P., BEE, J. & VON DER MARK, K. (1986). Transient expression of collagen type II at epitheliomesenchymal interfaces during morphogenesis of the cartilaginous neurocranium. *Devl Biol.* **116**, 497–509.

VON DER MARK, H., VON DER MARK, K. & GAY, S. (1976). Study of differential collagen synthesis during development of the chick embryo by immunofluorescence. I. Preparation of collagen type I

and type II antibodies and their application to early stages of the chick embryo. *Devl Biol.* **48**, 237–249.

WILL, L. A. & MELLER, S. M. (1981). Primary palatal development in the chick. *J. Morph.* **169**, 185–196.

YEE, G. W. & ABBOTT, U. K. (1978). Facial development in normal and mutant chick embryos: scanning electron microscopy of primary palate formation. *J. exp. Zool.* **206**, 307–322.

ZANETTI, M., RATCLIFFE, A. & WATT, F. M. (1985). Two subpopulations of differentiated chondrocytes identified with a monoclonal antibody to keratan sulphate. *J. Cell Biol.* **101**, 53–59.

(*Accepted 4 April 1989*)